

2-[(*cis*-2-methylcyclopropyl)acetoxy]-1,1,3,3-tetramethylisoindoline (5 mg); and (iii) a nonaromatic polar carbonyl compound (4 mg), possibly a carbonic anhydride.

2-[(2,2-Dimethylcyclopropyl)methoxy]-1,1,3,3-tetramethylisoindoline (6c): $^1\text{H NMR}$ (200 MHz, CDCl_3) δ 0.2 (m, 1 H), 0.6–1.1 (m, 2 H), 1.04 (s, 3 H), 1.09 (s, 3 H), 1.42 (br s, 12 H), 3.72 (m, 2 H), 7.01 (m, 2 H), 7.15 (m, 2 H). Anal. Calcd for $\text{C}_{18}\text{H}_{27}\text{NO}$: C, 79.07; H, 9.95. Found: C, 79.01; H, 9.64.

2-[(*cis*-2-Methylcyclopropyl)methoxy]-1,1,3,3-tetramethylisoindoline (6d^{cis}): $^1\text{H NMR}$ (200 MHz, CDCl_3) δ 0.3–1.0 (m, 4 H), 1.02 (m, 3 H), 1.44 (br s, 12 H), 3.74 (m, 2 H), 7.01 (m, 2 H), 7.14 (m, 2 H). Anal. Calcd for $\text{C}_{17}\text{H}_{25}\text{NO}$: C, 78.72; H, 9.71. Found: C, 78.46; H, 9.44.

2-[(*trans*-2-Methylcyclopropyl)methoxy]-1,1,3,3-tetramethylisoindoline (6d^{trans}): $^1\text{H NMR}$ (200 MHz, CDCl_3) δ -0.33 (m, 1 H), 0.10 (m, 1 H), 0.64 (m, 1 H), 0.86 (m, 1 H), 0.97 (d, 3 H, 6 Hz), 1.4 (br s, 12 H), 3.70 (d, 2 H, 6.8 Hz), 7.02 (m, 2 H), 7.16 (m, 2 H). Anal. Calcd for $\text{C}_{17}\text{H}_{25}\text{NO}$: C, 78.72; H, 9.71. Found: C, 78.61; H, 9.79.

2-(2-Methyl-3-buten-1-oxyl)-1,1,3,3-tetramethylisoindoline (5d): $^1\text{H NMR}$ (200 MHz, CDCl_3) δ 1.10 (d, 3 H, 7.2 Hz), 1.4 (v br d, 12 H), 2.22 (m, 1 H), 3.76 (d, 2 H, 7 Hz), 5.02 (m, 2 H), 5.82 (m, 1 H), 7.00 (m, 2 H), 7.11 (m, 2 H). Anal. Calcd for $\text{C}_{17}\text{H}_{25}\text{NO}$: C, 78.72; H, 9.71. Found: C, 78.76; H, 9.53.

2-(4-Penten-2-oxyl)-1,1,3,3-tetramethylisoindoline (7d): $^1\text{H NMR}$ (200 MHz, CDCl_3) δ 1.22 (d, 3 H, 7 Hz), 1.3–1.5 (m, 12 H), 2.19 (m, 2 H), 3.92 (sec, 1 H), 5.01 (m, 2 H), 5.81 (m, 1 H), 7.00 (m, 2 H), 7.11 (m, 2 H). Anal. Calcd for $\text{C}_{17}\text{H}_{25}\text{NO}$: C, 78.72; H, 9.71. Found: C, 79.01; H, 9.97.

2-[1-(Ethoxycarbonyl)-3-buten-1-oxyl]-1,1,3,3-tetramethylisoindoline (7e): $^1\text{H NMR}$ (200 MHz, CDCl_3) δ 1.28 (t, 3 H, 7 Hz), 1.2–1.5 (m, 12 H), 2.55 (m, 2 H), 4.17 (q, 2 H, 7 Hz), 4.40 (t, 1 H), 5.05 (m, 2 H), 5.75 (m, 1 H), 7.04 (m, 2 H), 7.19 (m, 2 H). Anal. Calcd for $\text{C}_{19}\text{H}_{27}\text{NO}_3$: C, 71.89; H, 8.57. Found: C, 71.80; H, 8.45.

Kinetic Experiments. For kinetic studies, reaction mixtures were made up volumetrically from common stock solutions, then degassed by the freeze/thaw method, and sealed in 1-mL Pyrex ampules.

Whenever possible, a series of reaction mixtures were heated simultaneously and analyzed under identical conditions. After completion of the reaction, the mixture was carefully evaporated, and the residue was dissolved in MeOH and analyzed by HPLC with isocratic elution ($\text{H}_2\text{O}/\text{MeOH}$; 1.3 mL/min). Trapped

products were detected by their UV absorption at 270 nm, identified by comparison of retention times with those of the authentic compounds, and quantified by integration of the chromatographic trace using the known extinction coefficients. Tests with mixtures of authentic samples showed the analytical precision to be better than 5% for yields and 3% for product ratios. The relative yields of substituted hydroxylamines obtained from the peroxide 4d at 60 °C are given in Table I. The ratios of yields from experiments conducted at 106 °C were as follows (data are given in the order [T] mM, 7c/5c, 6c/7c; nd = not determined): 256, 5.81, 0.052; 137, 6.39, 0.024; 106, 9.09, nd; 9.0, 29.4, nd.

From the peroxide 4d^{cis} at 59 °C, the relative yields of products 7d/5d and 6d^{cis}/7d were as follows: 273, 4.22, 0.33; 145, 4.23, 0.19; 71, 450, 0.075; 9.0, 4.51, nd; 4.5, 4.63, nd; 0.90, 5.60, nd. At 100 °C: 256, 3.65, 0.14; 138, 3.64, 0.073; 67, 3.94, 0.032; 9.0, 3.31, nd; 4.5, 4.51, nd; 0.85, 8.02, nd.

From the peroxide 4d^{trans} at 59 °C, the relative yields of products 7d/5d and 6d^{trans}/7d were as follows: 271, 1.15, 0.73; 143, 1.04, 0.39; 72, 1.10, 0.20; 9.0, 1.14, nd; 4.6, 1.22, nd; 0.84, 6.02, nd. At 100 °C: 255, 1.38, 0.18; 139, 1.42, 0.097; 67, 1.39, 0.050; 8.4, 1.53, nd; 4.2, 1.75, nd; 0.84, 3.03, nd.

Acknowledgment. We are indebted to Professor Martin Newcomb for making the results of his kinetic experiments available to use prior to publication.

Registry No. 1b, 120034-57-3; 1c, 87110-24-5; 1d, 52898-42-7; 2a, 2154-76-9; 2c, 90429-69-9; 2d^{cis}, 62131-98-0; 2d^{trans}, 62131-99-1; 2e, 118089-50-2; 4c, 120034-58-4; 4d^{cis}, 120034-61-9; 4d^{trans}, 120142-70-3; 4e, 120034-59-5; 5d, 120034-66-4; 6c, 120034-63-1; 6d^{cis}, 120034-64-2; 6d^{trans}, 120034-65-3; 7d, 120034-67-5; 7e, 120034-68-6; T, 80037-90-7; 2,2-dimethylcyclopropaneacetic acid, 68258-20-8; 2,2-dimethylcyclopropaneacetyl chloride, 120034-60-8; 3-pentyn-1-ol, 10229-10-4; 3-pentynoic acid, 36781-65-4; methyl 3-pentynoate, 22377-43-1; methyl *cis*-3-pentenoate, 36781-66-5; crotyl bromide, 4784-77-4; *trans*-pent-3-enitrile, 16529-66-1; *trans*-pent-3-enoic acid, 1617-32-9; methyl *trans*-pent-3-enoate, 20515-19-9; *trans*-2-methylcyclopropaneacetic acid, 54353-00-3; methyl *cis*-2-methylcyclopropaneacetate, 120142-68-9; methyl *trans*-2-methylcyclopropaneacetate, 120142-69-0; *tert*-butyl but-3-enoate, 14036-55-6; *cis*-2-(ethoxycarbonyl)cyclopropaneacetic acid, 120034-62-0; *trans*-2-(ethoxycarbonyl)cyclopropaneacetic acid, 120034-69-7.

Calculation of the Unusual NMR Chemical Shifts in Bicyclic Molecules Containing Strained Frameworks. A Simple Empirical Model for Predicting the Magnitude of the Anomalous Shift Increments

Charles F. Wilcox, Jr.*

Department of Chemistry, Cornell University, Ithaca, New York 14853-1301

Rolf Gleiter

Institut für Organische Chemie, Universität Heidelberg, D-6900 Heidelberg, West Germany

Received July 29, 1988

Many strained bicyclic and tricyclic alkenes and dienes show unusually large ^{13}C NMR shifts of the homoallylic carbons relative to the saturated reference compound, whereas the allylic carbons show only small shift increments. The direction of the homoallylic shift increment depends on whether the unsaturated bridge is a monoene or diene. Theoretical calculations with the Garber–Ellis INDO model for chemical shifts correctly reproduce the pattern of shift increments and identify them with variations in the local paramagnetic anisotropy. An empirical correlation between the shift increments and the change in carbon 2s population is demonstrated. A simple Hückel model for estimating the dependence of the shift increment on the structure of the bridge is presented.

Introduction

Christl et al.¹ reported that hydrocarbons containing a rigid cyclopentene ring give an unusually large downfield

^{13}C NMR shift of the homoallylic carbon atoms. For example, the ^{13}C NMR absorption of C-7 in norbornene (1) is shifted downfield by 9.8 ppm relative to C-7 in norbornane (2). With bicyclo[2.1.1]hexane (3) and bicyclo[2.1.1]hexane (4) the downfield shift increment of C-1, C-4

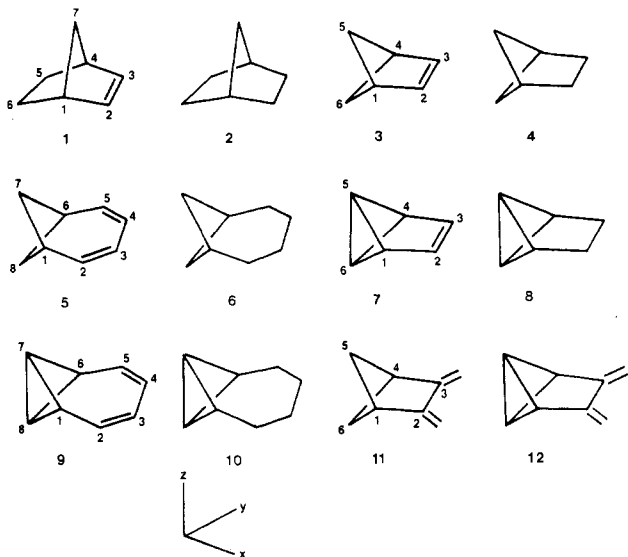
(1) Christl, M.; Herbert, R. *Org. Magn. Reson.* 1979, 12, 150.

Table I. Calculated and Observed ^{13}C NMR Chemical Shift Increments

hydrocarbon	carbon	obsd ^a	obsd increments		calcd increments	
			homoallylic ^b	allylic ^c	homoallylic ^b	allylic ^c
1	1, 4	41.8 ¹		-0.2		+7.6
	7	48.5 ¹	+9.8		+9.1	
2	1, 4	42.0 ¹		[0.0]		[0.0]
	7	38.7 ¹	[0.0]		[0.0]	
3	1, 4	42.9 ¹		+3.0		+8.2
	5, 6	68.0 ¹	+28.7		+17.4	
4	1, 4	39.9 ¹				
	5, 6	39.3 ¹				
7	1, 4	36.6 ³		+2.6		+11.7
	5, 6	48.3 ³	+45.9		+36.5	
8	1, 4	34.0 ³				
	5, 6	2.4 ³				
5	1, 6	35.2 ³		+0.9		+5.2
	7, 8	21.6 ³	-8.5		-8.7	
6	1, 6	34.3 ³				
	7, 8	30.1 ³				
9	1, 6	45.3 ³		-8.1		-3.8
	7, 8	-13.4 ³	-23.9		-24.7	
10	1, 6	53.4 ³				
	7, 8	10.5 ³				
11	1, 4					+7.8 ^d
	5, 6	43.8 ⁶	+4.4		-0.4	
12	1, 4					+7.5 ^e
	5, 6	11.7 ⁶	+9.3		+3.5	

^a Relative to TMS in ppm. ^b Difference between the saturated and unsaturated shifts at carbons 5, 6 or 7, 8 in ppm. ^c Difference between the saturated and unsaturated shifts at carbons 1, 4 or 1, 6 in ppm. ^d Relative to hydrocarbon 4. ^e Relative to hydrocarbon 8.

in the unsaturated hydrocarbon is 28.6 ppm. The bridgehead carbons of 1 and 3, which are adjacent to the double bond and might be expected to be more affected, show little shift compared to the bridgehead carbons of 2 and 4. In striking contrast to this "norbornene effect" or "cyclopentene effect" the homoallylic C-7, C-8 carbons of compounds with the bicyclo[4.1.1]octa-2,4-diene skeleton, e.g. 5, show marked *upfield* shift² of 16.2 ppm relative to the same carbons in the saturated bicyclic hydrocarbon, e.g. 6 (see Table I). In all of these hydrocarbons the protons attached to the homoallylic carbons show anomalous shifts in the same direction as the the carbon increments, although the magnitude is much smaller.



Extensive preparative and spectroscopic studies by the Christl,³ Gleiter,⁴ and Paquette⁵ groups have greatly ex-

tended the range of hydrocarbons showing anomalous homoallylic shift increments. It is now clear that the pattern is the following: (a) the phenomenon occurs in strained hydrocarbons; (b) only the homoallylic carbons (and attached hydrogens) show significant shifts; (c) a two-carbon monoene bridge causes a *downfield* shift and a four-carbon diene bridge causes an *upfield shift*; and (d) an interruption of the conjugation results in no anomalous shift. A selection of the observed shift increments is presented in columns 5 and 6 of Table I.

Origin of the Anomalous Shift Increments

Over the years, as the facts accumulated, a number of hypotheses to explain the phenomenon were put forward. Christl and Herbert¹ originally proposed that the homoallylic upfield shift increments of C-5, C-6 in 3 resulted from charge shifts from these carbons to the LUMO of the double bond. Sander and Gleiter² noted that MINDO/3, MINDO, and EHT calculations all failed to predict any charge shift for either 3 or 5. Instead, they proposed that the shift increments were connected with the differing local anisotropies of the two- and four-carbon olefinic bridges. Christl and Herzog³ then reported analogous, but larger, downfield shift increments for tricyclo[3.1.0.0^{2,6}]hex-3-ene and the related saturated hydrocarbon 8 as well as larger upfield shift increments for tricyclo[5.1.1.0^{2,8}]oct-3,5-diene (9) and the related saturated hydrocarbon 10. They suggested that the larger shift increments observed for 7 and 9 were inconsistent with the Sander-Gleiter hypothesis since the presumed larger distances between the homoallylic carbons and the unsaturated bridges of 7 and 9 would predict the opposite. Christl and Herzog³ observed that the magnitude of the shift decreases with diminished strain of the cyclobutane ring, which they attributed to variations in the local paramagnetic anisotropy term to which the energies of the unoccupied MO's contribute.

(2) Sander, W.; Gleiter, R. *Chem. Ber.* 1985, 118, 2548.

(3) Christl, M.; Herzog, C. *Chem. Ber.* 1986, 119, 3067.

(4) Gleiter, R.; Sander, W.; Butler-Ranshoff, I. *Helv. Chim. Acta* 1986, 69, 1872. Gleiter, R., Mueller, G. *J. Org. Chem.* 1988, 53, 3912.

(5) Dressel, J.; Pansegrau, P.; Paquette, L. A., to be published.

(6) Schwager, L.; Vogel, P. *Helv. Chim. Acta* 1980, 63, 1176; 1982, 23, 2647.

Paquette⁵ confirmed the strain argument of Christl and Herzog within the diene series and attributed it to the lowering of the energy of the σ MO's. A hint of a similar correlation occurs with the monoenes, but it is much less marked.

In order to gain insight into the origin of this phenomenon, we have carried out magnetic anisotropy calculations for several of these strained hydrocarbons using the Garber–Ellis model.⁷ This model is based on an INDO formalism using gauge-invariant atomic orbitals with special parameters selected to fit ¹³C NMR hydrocarbon shifts. This model includes the diamagnetic and paramagnetic one-, two-, and three-center contributions to the shielding constants. Although the ¹³C NMR shifts calculated by this model are not highly accurate in an absolute sense, the trends accompanying structural variations were faithful enough for Garber et al. to identify the physical origins of many of the empirical correlations known to NMR spectroscopists. It was in this spirit that the model was applied to the present problem.

The structures used in the magnetic calculations were the fully optimized C_{2v} structures calculated by MINDO/3 model.⁸ The chemical shifts calculated by the Garber–Ellis program for the allylic and homoallylic carbons of these structures are recorded in Table I. From a comparison of columns 4 and 5 of Table I with columns 6 and 7, it is apparent that the pattern of chemical shift increments is reproduced quite faithfully. The homoallylic shift increments show the critical sign reversal between ethylene and butadiene bridges and even have the proper magnitudes. The magnitudes of the allylic shift increments are somewhat too positive (the model overestimates the inductive effect of adding an adjacent sp^2 center), but like the real system the calculated allylic shift increments have only a small dependence on the bridge size.

Given the success of the Garber–Ellis model, the next question is what is the origin of the anomalous homoallylic shift increments. As noted in above, the Garber–Ellis model includes the diamagnetic and paramagnetic contributions of the one-, two-, and three-center terms. There are a total of eight different contributions for each carbon atom: $\sigma_A^{d,AA}$, $\sigma_A^{p,AA}$, $\sigma_A^{d,AB}$, $\sigma_A^{p,AB}$, $\sigma_A^{d,BB}$, $\sigma_A^{p,BB}$, $\sigma_A^{d,BC}$, $\sigma_A^{p,BC}$, where the superscript XY and subscript A indicates the contribution to the chemical shift of nucleus A of current flows between orbitals on atom X and orbitals on atom Y; the superscript d and p indicate whether it has a diamagnetic or paramagnetic origin (ground-state effect or mixing of excited states). For example, the $\sigma_A^{p,BC}$ term is the paramagnetic contribution to the shielding of atom A due to current flows between orbitals on atoms B and C, which when combined with the corresponding diamagnetic terms give rise to the well-known "ring current" effects. When the eight terms were compared for each pair of related hydrocarbons (e.g., 1 and 2), it became clear that the main source of the anomalous shift increments was the variation in the paramagnetic terms $\sigma_A^{p,AA}$. This means that the effect of the ethylene and butadiene bridges is *not* due to differences in neighboring anisotropies ($\sigma_A^{d,p,BB}$) nor to ring currents ($\sigma_A^{d,p,BC}$ and $\sigma_A^{d,p,AB}$) involving these bridges; it also means that the shift increments are *not* due to changes in electron density on the homoallylic carbons ($\sigma_A^{d,AA}$). That the dominant term proved to be $\sigma_A^{p,AA}$ is not too surprising since it is this term that generally accounts for most ¹³C NMR chemical shift differences.⁹

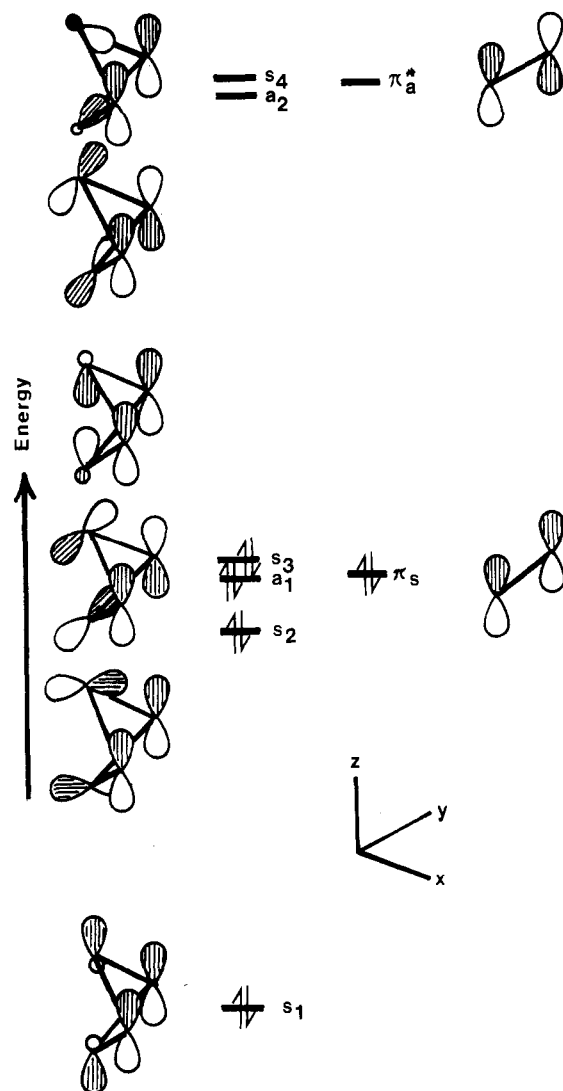


Figure 1. Interaction diagram for magnetic shifts in hydrocarbon 3.

The classical picture associated with the paramagnetic term, $\sigma_A^{p,AA}$, is that it represents the inhibition of the free circulation of electrons on atom A. Closer inspection of the diagonal tensor components of the $\sigma_A^{p,AA}$ terms (available as part of the computer printout) revealed that most of the variation arises in the zz component (see structure drawings for the coordinate axes orientations). Thus in classical terms the variations of the shift increments has to do with the variations in the inhibition of free circulation of electrons in the xy plane at the bridge carbons.

In order to understand why the different sizes of alkene bridges have different effects on $\sigma_A^{p,AA}$, it is necessary to consider both the *electrostatic* perturbation of the bridge orbitals and the changes these perturbations make on the response of the system to a *magnetic* perturbation.¹⁰ Figure 1 shows such a diagram appropriate for the ethylene-bridged hydrocarbon 3. In this diagram the only cyclobutane orbitals shown are those that have the proper asymmetry to interact with the π orbitals of the ethylene bridge; the hydrogen orbitals are now shown. Many of the

(7) Garber, A. R.; Ellis, P. D.; Seidman, K.; Schade, K. *J. Magn. Reson.* 1979, 34, 1–30.

(8) Bingham, R. C.; Dewar, M. J. S.; Lo, D. H. *J. Am. Chem. Soc.* 1975, 97, 1285, 1294.

(9) Levy, G. C.; Lichter, R. L.; Nelson, G. L. *Carbon-13 Nuclear Magnetic Resonance Spectroscopy*, 2nd ed.; Wiley: New York, 1980; p 31.

(10) Salem, L. *The Molecular Orbital Theory of Conjugated Systems*, Benjamin: New York, 1966.

missing levels make contributions to the total magnetic anisotropy, but these contributions do not change under the influence of the alkene perturbations and hence do not contribute to the shift increments.

The cyclobutane and ethylene orbitals can be classified according to their symmetry with respect to the xz plane and these are indicated in Figure 1 as s or a . On electrostatic perturbation of the cyclobutane orbitals by the ethylene orbitals the cyclobutane a_1 orbital acquires π_a^* density and the ethylene bridge π_s orbital acquires s_4 density. Because of the similarity of the orbital energies

$$\Psi_{\pi_s} = \frac{1}{(1 - A^2)^{1/2}} (\pi_s + A s_4)$$

$$\Psi'_a = \frac{1}{(1 - B^2)^{1/2}} (a_1 + B \pi_a^*)$$

$$A \approx B$$

and the magnitudes of the p_z coefficients on the bridge carbons, the amount of mixing is similar and there is little net electron transfer, as earlier quantum mechanical calculations had shown.² The net effect of the interaction is to transfer p_y electron density from the bridge carbons of the cyclobutane ring into p_x electron density on the same carbons; the bridgehead carbons are relatively unaffected because the two interactions essentially cancel at these positions. Another consequence of the electrostatic perturbation is that p_y electron density is also converted into $2s$ density on the same carbon. This has little effect on the shift increments ($2s$ orbitals are unresponsive to magnetic perturbations), but the $2s$ change in $2s$ density serves as a convenient probe of the electrostatic perturbation as will be described in the next section.

The zz component of the local paramagnetic shift anisotropy is determined by the magnetically induced mixing of the p_x and p_y orbitals between the ground and excited states. Mathematically, this cross interaction results because the magnetic operator converts a p_x orbital into a p_y orbital and vice versa. The amount of mixing will depend on the product of the p_x coefficient in one state and the p_y coefficient in the other, and, of course, the intensity of the magnetic field at the nucleus as well as the energy gap between the two states. The total effect is the sum over all pairs of ground and excited states. In the present case the coefficients are such that loss of p_x character and gain of p_y character leads to a net increase in the paramagnetic anisotropy at the bridge carbon, which results in a downfield shift of that carbon.

From the analogous perturbation diagram for the butadiene-bridged hydrocarbon, the conclusion is exactly the opposite because now the HOMO has a symmetry and the LUMO has s symmetry. Consequently, there is a net transfer of p_y density into p_x density, which leads to diminished paramagnetic anisotropy and an upfield shift increment. The shift increments are not as large with **5** as with **3** because in the butadiene-bridged hydrocarbon there are lower and higher lying π orbitals that have smaller but contrary effects.

In hydrocarbon **11** the shift increment is almost zero because now the HOMO and LUMO have small coefficients at the points of attachment to the bridgehead carbons, while the higher and lower lying orbitals have larger coefficients. The reversal in coefficient magnitude just about compensates for the differences in the energy gaps and there is little net change in the paramagnetic anisotropy.

With hydrocarbons **7** and **9** the same analysis applies, but with these compounds the change in orbital coefficients produces larger effects.

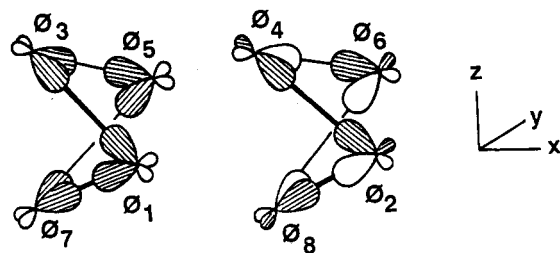


Figure 2. Basis set hybrid orbital combinations.

As Christl et al.³ and subsequently Paquette et al.⁵ have already concluded from experimental observations, the general magnitude of the shift increment depends on the magnitude of the mixing of the strained cyclobutane σ orbitals with the π alkene orbitals. The strain of the cyclobutane ring elevates the energy of the σ orbitals to a point where they can effectively interact with the π orbitals. The calculations and interpretation presented in this paper fully confirm their suggestions.

A detailed analysis of the proton shifts of the bridge protons has not been made, but they appear to be consistent with the changes in the paramagnetic anisotropy of the carbons to which they are attached.

A Correlation of Shift Increment with $2s$ Electron Density

In the perturbation analysis described in the previous section, it was noted that one effect of an ethylene bridge is to convert p_y electron density into $2s$ electron density; a butadiene bridge has the opposite effect. A plot of the calculated change in $2s$ electron density on substitution of the unsaturated bridge against the homoallylic shift increment accompanying the same substitution gives a fairly good linear relationship.

$$\text{shift increment} = 4.4 + 1115.6(\text{change in } 2s \text{ population})$$

The standard deviation in the shift increments (observed range of 70 ppm) was 7.5 ppm. It should be emphasized that the change in $2s$ population is not a direct cause of the shift increment but only a measure of how well a given alkene bridge induces changes of the p_x , p_y populations of the bridge carbons. A similar correlation can be obtained from the difference in the p_x , p_y populations, but the $2s$ correlation is more convenient because it is independent of molecular orientation.

A Simple Model for Predicting the Magnitude of the Anomalous Shift Increments

It is possible to construct a simple Hückel model for gauging the effect of various unsaturated bridges on the bicyclo[2.1.1]hydrocarbons. Several parameter schemes were explored, but they all led to essentially the same conclusion regarding the effect of structure. The scheme presented here is short on physical realism, but it works and has the virtue of simplicity. The cyclobutane ring is modeled as a set of eight local hybrid atomic orbitals that have been combined pairwise to accommodate the p_y and p_z symmetry required to complement the perturbation analysis (see Figure 2). For example, orbital 1 is taken as the sum of two sp^3 -hybridized orbitals on C_1 with one hybrid pointing toward C_2 and the other toward C_4 . The combination is an sp^2 hybrid that lies in the yz plane and is orthogonal to a p_z orbital at C_1 . As a second example, orbital 4 on C_2 is a similar sum of two hybrid orbitals, but with opposite phases, so that the combination is parallel to the y axis.

For the Hückel calculations all β s between orbitals on the same carbon were taken to be zero and the β s between orbitals on adjacent carbons were taken to be ± 0.5 with the sign determined by whether the overlap was between lobes of the same sign ($\beta = -0.5$) or of opposite sign ($\beta = +0.5$). The β s for the p_z orbitals on the unsaturated moiety were taken to be -1.0 in the usual Hückel fashion as were the β s between the points of attachment of the unsaturated moiety to orbitals 2 and 6 on carbon atoms 1 and 2. The β s for interaction with orbitals 1 and 5 were taken to be zero by reason of symmetry.

The electron density calculated for cyclobutane by this model is unity for all orbitals. With hydrocarbon 3 the calculated population of orbital 3 grows at the expense of orbital 4. The other orbital populations stay the same. With hydrocarbon 7 it is orbital 4 that grows at the expense of orbital 3. With hydrocarbon 11 there is only a small change in the densities of orbitals 3 and 4. These results qualitatively parallel the conclusions drawn from the full INDO calculations and their perturbation analysis. The quantitative relationship between the observed shift increments and the calculated difference in orbital 3 and orbital 4 populations, while less than perfect, are hopefully good enough to identify hydrocarbons with potentially interesting shifts. The equation and a few of the predictions made with it are shown below.



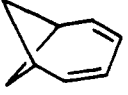

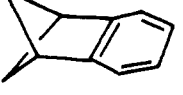
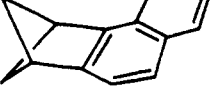
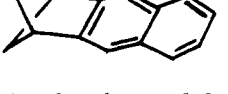
$$\text{shift increment} = 4.2 +$$

$$71.1(\text{population of orbital 3} - \text{population of orbital 4})$$

$$\text{average error} = 3.4 \text{ ppm}$$

Conclusions

The anomalous shift increments for these strained bicyclic and tricyclic alkenes arise from variations in the local paramagnetic anisotropy term. The sign and magnitude of the shifts can be analyzed in terms of joint *electrostatic* and *magnetic* perturbations. An empirical correlation between the shift increments and changes in carbon 2s population is noted. A simple Hückel-based model ac-

	$P_3 - P_4$	shift
	0.000	0.0
	+0.301	+28.7
	-0.229	-8.5
	+0.040	+4.4
	+0.169	+16.2*
	+0.201	+18.5*
	+0.128	+13.3*

* predicted

counts for the observed dependence of the shifts on the structure of the unsaturated bridge.

Acknowledgment. We thank P. Bischof for calculating several of the MINDO/3 geometries. The work was facilitated by an Alexander von Humboldt award to C. F. Wilcox, Jr.

[2 + 4] Photocyclization between Quinones and Allenes via Photoinduced Electron Transfer

Kazuhiro Maruyama* and Hiroshi Imahori

Department of Chemistry, Faculty of Science, Kyoto University, Kitashirakawa, Sakyo-ku, Kyoto 606, Japan

Received November 15, 1988

Photochemical reactions of halo-1,4-naphthoquinones with 1,1-diphenylallenes afforded spiropyran adducts derived from [2 + 4] cycloaddition between carbonyl group of quinone and allene in good yield. In the photoreactions of 2,3-dichloro-1,4-naphthoquinone with monophenylallenes, [2 + 2] cycloadducts were obtained in addition to spiropyran derivatives. Considering the relationship between formation of spiropyran adducts and the free energy changes (ΔG) together with substituent effects, solvent effects, and CIDNP (chemically induced dynamic nuclear polarization), we propose an electron-transfer mechanism. That is, radical ion pair formation from excited triplet quinone and allene is followed by conversion to a biradical. Subsequent bond formation between the ketyl radical in quinone moiety and ortho positions of the phenyl substituents on the allene skeleton leads to the spiropyran adduct after subsequent 1,5-hydrogen shift.

Since about 20 years ago we have been engaged into the photochemistry of quinones to explore novel photochemical reactions.¹ Specifically, photochemical reactions of

halo-1,4-naphthoquinones with 1,1-diphenylethylenes have been extended remarkably.² The reactions proceed by substitution of a halogen atom with the ethylenic group (ethylene adduct), and subsequent photocyclizations result

(1) (a) Bruce, J. M. In *The Chemistry of the Quinonoid Compounds*; Patai, S., Ed.; John Wiley & Sons: New York, 1974; Vol. 1, Part 1, Chapter 9. (b) Maruyama, K.; Osuka, A. In *The Chemistry of the Quinonoid Compounds*; Patai, S., Rappoport, Z., Eds.; John Wiley & Sons: New York, 1988; Vol. 2, Part 1, Chapter 13, and references therein.

(2) (a) Maruyama, K.; Otsuki, T. *Chem. Lett.* 1975, 87. (b) Maruyama, K.; Otsuki, T.; Mitsui, K. *J. Org. Chem.* 1980, 45, 1424. (c) Maruyama, K.; Otsuki, T.; Tai, S. *Ibid.* 1985, 50, 52.